Rabi Oscillations in a Josephson-Junction Charge Two-Level System

Y. Nakamura,[1] Yu. A. Pashkin,[2,*] and J. S. Tsai[1]

[1]*NEC Fundamental Research Laboratories, Tsukuba, Ibaraki 305-8501, Japan*
[2]*CREST, Japan Science and Technology Corporation (JST), Kawaguchi, Saitama, 332-0012, Japan*
(Received 24 October 2000; published 27 November 2001)

We investigated temporal behavior of an artificial two-level system driven by a strong oscillating field; namely, quantum-state evolution between two charge states in a small Josephson-junction circuit irradiated with microwaves. Rabi oscillations corresponding to 0-, 1-, and 2-photon resonances were observed. As a function of microwave amplitude, the Rabi frequencies followed a first-kind Bessel function of the corresponding order to the number of photons.

A two-level system is a simple model widely applied to many problems in physics. For decades, time evolution of the quantum states of a two-level system has been extensively studied in many contexts; for example, nonadiabatic transition at the level crossing [1], quantum-state evolution under a resonant driving field (Rabi oscillations) [2], and the effect of dissipative environment coupled to the two-level system [3]. Moreover, recent proposals for implementations of quantum computation [4], which require coherent control of the quantum state of a two-level system, i.e., a qubit, have enhanced the interest in the dynamic behavior of a two-level system under a driving force such as an oscillating field or a high-speed pulse field [5].

One of the candidates for physical realization of a qubit is a small Josephson-junction circuit called a Cooper-pair box, which consists of a small superconducting electrode connected to a reservoir via a Josephson junction [6]. Because of the charging effect of the small electrode, two charge-number states, in which the number of Cooper pairs in the "box" electrode differs by one, constitute an effective two-level system. Because of the collective nature of the superconducting state, the two-level system is basically characterized simply by "macroscopic" parameters, the Josephson energy and the charging energy, which can be well controlled by the geometry of the circuit designed and fabricated by present nanotechnology. Superposition of the two charge states has been confirmed in experiments [7,8], and coherent manipulation of the quantum state by using a dc gate-voltage pulse has been demonstrated; i.e., coherent oscillations between two degenerate charge states were observed [9].

In this Letter, we demonstrate an alternative way of coherent control using a microwave field [10] and we report the observation of Rabi oscillations; the quantum state of the system evolves in an oscillatory manner between two nondegenerate charge states in resonance with the driving field. Although Rabi control of quantum states is very popular in microscopic systems such as atoms [11] and spins [12] as a standard method of qubit operation, to our knowledge, our result is the first demonstration of Rabi control in a single artificial two-level system in a solid-state device. Furthermore, a strongly driven regime, where higher-order

interactions between the two-level system and the coherent external field become important, is realized in the present experiment. We observe expected Bessel-function power dependence of the Rabi frequency.

Rabi oscillation dynamics in our experiment is reduced into a simple model Hamiltonian, $H = \frac{1}{2}\hbar\omega_0\sigma_z + \frac{1}{2}\hbar\omega_1\sigma_x + \hbar\omega a^\dagger a + g\sigma_z(a + a^\dagger)$, where $\sigma_i(i = x, y, z)$ is the Pauli spin matrices and a, $a^\dagger$ are the creation and annihilation operators for a field mode with an angular frequency of ω. The first two terms characterize the two-level system with energy asymmetry $\hbar\omega_0$ and tunneling matrix element $\hbar\omega_1$. The third and fourth terms represent the driving field and its coupling to the two-level system; g is the coupling constant.

Under the limit $N \simeq \langle N \rangle \equiv \langle a^\dagger a \rangle \gg 1$, the Hamiltonian matrix can be written as [$J_m \equiv J_m(\alpha)$ is the first-kind Bessel function of mth order]

$$\begin{pmatrix} \ddots & & & & & \ddots \\ & E_{N+1}^- & \frac{\hbar\omega_1}{2}J_1 & 0 & \frac{\hbar\omega_1}{2}J_2 & \\ & \frac{\hbar\omega_1}{2}J_1 & E_N^+ & \frac{\hbar\omega_1}{2}J_0 & 0 & \\ & 0 & \frac{\hbar\omega_1}{2}J_0 & E_N^- & \frac{\hbar\omega_1}{2}J_1 & \\ & \frac{\hbar\omega_1}{2}J_2 & 0 & \frac{\hbar\omega_1}{2}J_1 & E_{N-1}^+ & \\ \ddots & & & & & \ddots \end{pmatrix}.$$

Here we use the dressed-state basis derived for $\omega_1 = 0$ [13],

$$|\pm; N\rangle_{\text{dressed}} = \exp[\mp g(a^\dagger - a)/\hbar\omega]|\pm\rangle|N\rangle,$$

and their eigenenergies $E_N^\pm \equiv N\hbar\omega - g^2/\hbar\omega \pm \frac{1}{2}\hbar\omega_0$, where $|\pm\rangle$ are eigenstates of σ_z, and $\alpha \equiv 4g\sqrt{\langle N\rangle}/\hbar\omega$ is a scaled amplitude of the driving field. When $E_{N+m}^- \simeq E_N^+$, that is, when $m\hbar\omega \simeq \hbar\omega_0$, the two dressed states show anticrossing due to the off-diagonal coupling $\frac{\hbar\omega_1}{2}J_m(\alpha)$. Thus, if we prepare a localized initial state in the σ_z basis, Rabi oscillation takes place, and the Rabi frequency is expected to be $|\omega_1|J_m(\alpha)$ [14]. The dressed-state approach, in contrast to the lowest-order perturbation approach that gives only 1-photon Rabi frequency linearly depending on α, takes into account all the higher-order processes involving net m photons and, thus, is applicable even to a strongly driven regime.

The similarity and the difference between the Rabi oscillations and the standard ac Josephson effect are readily understood. Under an ac driving field, a voltage-biased large Josephson junction with negligible charging energy shows microwave-induced Josephson current (in Shapiro steps) which also follows Bessel functions of the field amplitude [15]. In the charge-state representation, the situation can be modeled with a driven tight-binding array of charge-number states, which is tilted by a dc bias voltage [5]. The height of the Shapiro step is proportional to the microwave-induced matrix element between the nearest-neighbor charge states, that is, the width of the microwave-induced energy band in the one-dimensional array. On the other hand, when the charging effect is increased, the number of available charge states decreases due to the quadratic confinement potential in the charge space, and finally becomes two as in a Cooper-pair box, in which we observe Rabi frequency as a measure of the microwave-induced matrix element between two charge states.

A schematic of the Cooper-pair box circuit is shown in Fig. 1(a). The sample was fabricated by electron-beam lithography and shadow evaporation of Al films. The box electrode is coupled to the reservoir via a Josephson junction, which has Josephson energy E_J, and is coupled capacitively to two gate electrodes (dc and pulse), which modulate the energy of the charge states $|n\rangle$ as $4E_C(n - Q_t/2e)^2$. Here, n is the excess number of Cooper pairs in the box, $Q_t \equiv C_g V_g + C_p V_p + C_b V_b$ is the total gate-induced charge, $E_C \equiv e^2/2C_\Sigma$ is the single-electron charging energy, and C_Σ is the total capacitance of the box. C_i ($i = g, p, b$) is the capacitance between the box and each electrode, on which voltage V_i is applied. An additional voltage-biased probe electrode is attached to the box via a highly resistive ($R_b \sim 53$ MΩ) tunnel junction for the measurement of the charge state (see below). The sample was mounted in a shielded package at the base temperature of a dilution

refrigerator ($T \sim 30$ mK; $k_B T \sim 3$ μeV). From data sets of current-voltage characteristics between the reservoir and the probe for various dc gate voltages, we estimated the superconducting gap energy of the electrodes Δ as 250 ± 10 μeV. With photon-assisted Cooper-pair tunneling spectroscopy [8], E_J and E_C were estimated to be 30 ± 5 μeV and 280 ± 5 μeV, respectively.

Because of the large E_C, charge states with large $|n - Q_t/2e|$ become energetically unfavorable. Also, the large Δ suppresses quasiparticle excitations. Thus, at low enough temperatures, the device can be considered an effective two-level system by taking into account only the two lowest-energy charge states, which differ by one Cooper pair. In the following, we focus on the two charge states $|0\rangle$ and $|1\rangle$ without losing generality. In this truncated Hilbert space ($|0\rangle$ as $|-\rangle$ and $|1\rangle$ as $|+\rangle$), correspondence to the model Hamiltonian above is $\hbar\omega_0 = \delta E(Q_t) \equiv 4E_C(Q_t/e - 1)$, where δE is the charging energy difference between the two states, $\hbar\omega_1 = -E_J$, $\hbar\omega = hf$, and $\alpha \equiv 4g\sqrt{\langle N \rangle}/\hbar\omega = (2eV_{ac}/hf)(C_p/C_\Sigma)$, where f and V_{ac} are the frequency and amplitude of continuous-wave (cw) microwaves applied at the pulse gate (see below).

Figures 1(b) and 1(c) illustrate the scheme of our quantum-state control via Rabi oscillations. The quantum state of the two-level system is controlled by using a fast dc gate-voltage pulse which modulates the energy levels of the two-level system and therefore modulates the resonant condition between a cw microwave and the two-level system. For that purpose, we add a cw microwave with a frequency f and a dc pulse with a length of Δt (minimum pulse length is 80 ps; rise and fall times are 30–40 ps) [Fig. 1(c)], and feed the signal from the sources at room temperature to the open-ended pulse gate through a low-loss coaxial line and an on-chip coplanar line. The details of the experimental setup are described elsewhere [16]. The phase of the cw microwave is not locked to the pulse signal. In the present experiment, hf is larger than E_J.

Suppose for the initial state that $Q_0 \equiv C_g V_g + C_b V_b$ is much smaller than $1e$ and the system is prepared in the ground state $\sim |0\rangle$ [black circle in Fig. 1(b)]. In this state, the frequency of the microwaves applied to the pulse gate does not match the energy gap and thus does not couple to the two-level system. The overlapping dc pulse abruptly shifts the energy levels to the m-photon resonance point (gray circles); Rabi oscillations with an angular frequency $\Omega_{\text{Rabi},m}$ start and last for the pulse duration Δt, where m is the number of net photons involved in the transition. After the pulse, the state of the system becomes a superposition of the two charge states (black and white circles) with a weight depending on the phase of the oscillations.

The measurement of the final state is conducted by using the voltage-biased probe junction. Under an appropriate bias condition, state $|1\rangle$ decays into $|0\rangle$ via two sequential single-electron (quasiparticle) tunneling processes through the probe junction with finite rates Γ_{qp1} and Γ_{qp2}, while $|0\rangle$ is stable [9]. Although it is difficult to
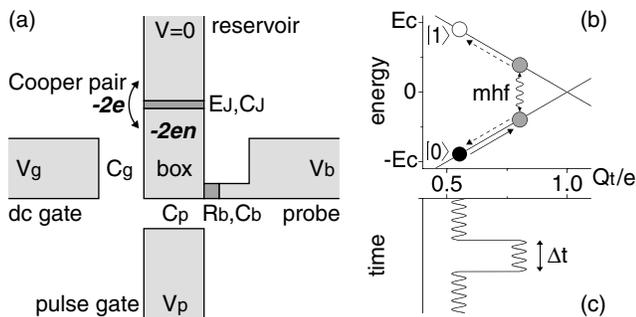
FIG. 1. (a) Schematic of a Cooper-pair box and an additional probe electrode. (b) Control of the quantum states using Rabi oscillations. The solid lines represent relative energies of two charge states $|0\rangle$ and $|1\rangle$ as a function of total gate-induced charge Q_t. Black circle: initial state. Gray circles: two states under Rabi oscillations. The final state is a superposition of the two states shown by black and white circles. (c) Schematic waveform of the voltage applied to the pulse gate.

detect the two electrons in a single trial, we can rapidly repeat the same pulse operations and measurements with a repetition time $T_r(>1/\Gamma_{qp1} + 1/\Gamma_{qp2})$ to obtain a dc probe current corresponding to the population of $|1\rangle$ in the final state. Since the probe is always connected to the system, $1/\Gamma_{qp1}$ must be longer than the time scale of the Rabi oscillations in order not to disturb the coherence too much. In the present experiment with a fixed probe voltage $V_b = 850 \ \mu$V, $1/\Gamma_{qp1}$ and $1/\Gamma_{qp2}(\propto R_b)$ were estimated from Fermi's golden rule to be about 7.9 and 18 ns.

Figure 2 shows the current through the probe junction, I, as a function of Q_0. Since we could not know beforehand the height of the actual pulse at the pulse gate, we swept the baseline of the pulse, i.e., Q_0, with a fixed pulse height. Without using microwave or pulse modulation [Fig. 2(a)], a single broad resonant-tunneling peak can be seen at $Q_0/e = 1$ where two charge states are degenerate. The sudden drop of the current at $Q_0/e \simeq 1.1$ is caused by the suppression of the quasiparticle-tunneling rate Γ_{qp2} due to the superconducting gap in the density of states; therefore, our measurement scheme does not work at higher Q_0. Under cw microwaves with a frequency f of 20 GHz and a relative power A of -6 dB [Fig. 2(b)], photon-assisted tunneling-current peaks appear (three photon-absorption peaks at $Q_0/e < 1$ and a weak photon-emission peak at $Q_0/e > 1$) [8]. The short-dashed lines show the peak positions calculated by using the sample parameters. By applying a pulse array with $\Delta t = 80$ ps and $T_r = 64$ ns [Fig. 2(c)], the pulse-induced current due to the coherent oscillations between two charge states shows an oscillating behavior as a function of Q_0 [9]. The pulse height at the pulse gate was estimated from a series of I-Q_0 curves with various Δt; we found that the states prepared

at $Q_0/e \simeq 0.63$ (indicated by the long-dashed line) were brought into the exact degeneracy point during the pulse duration. By combining the cw and pulse modulations [Fig. 2(d)], an extra peak in the I-Q_0 curve, as indicated by an arrow, appears. The spacing from the long-dashed line is almost the same as that corresponding to the microwave photon energy hf and turned out to be proportional to f (data not shown), suggesting that this peak is due to the Rabi process with $m = 1$ shown in Fig. 1(b). At higher microwave power, more peaks appeared, corresponding to processes with larger m [Fig. 2(e)].

The measurement in the time domain was done by changing pulse length Δt. Figure 3(a) shows the peak current due to the 1-photon Rabi process [see Fig. 2(d)] as a function of Δt for various microwave powers. We observe Rabi oscillations whose frequency depends on microwave power A, and the oscillation frequency changes nonmonotonously as a function of A. Similar oscillations can also be seen for $m = 0$ and 2 [Fig. 3(b)]. Although the details on the decoherence of the driven two-level system is out of the scope of this paper, some of the oscillations continue nearly up to 2 ns.

We mention that the peak current in the I-Q_0 curves is plotted here instead of the current at a fixed Q_0 (cf. Ref. [9]). The latter procedure did not work in the present experiment, since the curves were randomly shifted as well as smeared by small fluctuations of Q_0, which were presumably due to the random motions of background charged impurities distributed around the device. In contrast, the former procedure is confirmed through numerical simulations to be useful in obtaining the oscillation periods even in the presence of moderate fluctuations of Q_0. This choice of procedure also explains the small amplitude and the large background current in
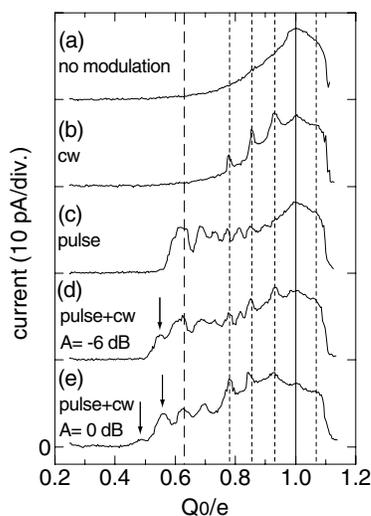
FIG. 2. Current through the probe junction as a function of Q_0: (a) without microwave or pulse irradiation, (b) with microwave, (c) with pulse, and (d),(e) with both microwave and pulse. Microwave frequency f is 20 GHz. Pulse length Δt and repetition time T_r are 80 ps and 64 ns.
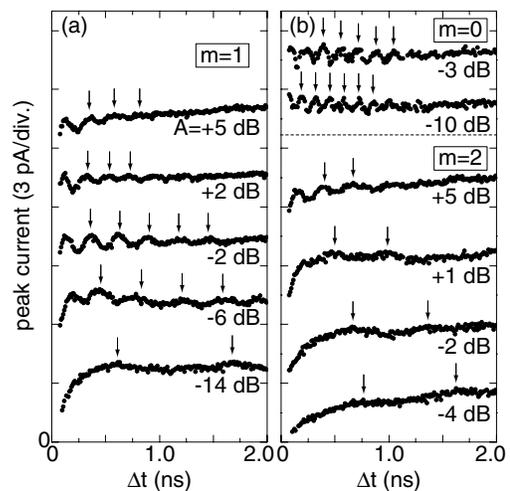
FIG. 3. m-photon Rabi oscillations observed in the relevant peak current in I-Q_0 curves [see Figs. 2(d) and 2(e)] as a function of pulse length Δt. (a) for $m = 1$ and (b) for $m = 0$ and 2. The arrows indicate the period of the oscillations. Each result for different microwave power A is shifted vertically by 3 pA for clarity.
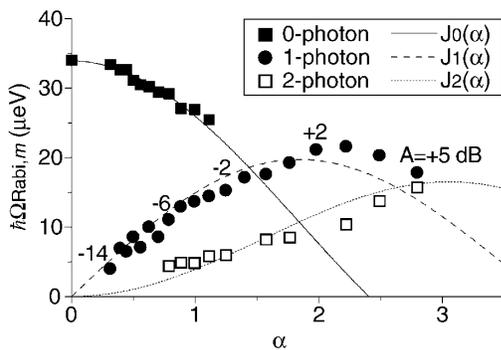
FIG. 4. Rabi-oscillation frequency $\Omega_{\text{Rabi},m}$ ($m = 0$, 1, and 2, respectively, for 0-, 1-, and 2-photon processes) as a function of irradiated microwave amplitude. Lines are the first-kind Bessel functions of the corresponding order, $J_m(\alpha)$, where $\alpha \equiv (2eV_{\text{ac}}/hf)(C_p/C_\Sigma)$.

Fig. 3. If it were phase locked, combined pulse and cw modulations could result in complicated oscillations in the time domain, involving a Rabi component and the cw carrier component. However, in the present experiment, the result was averaged over the phase shift between the pulse and the cw microwaves.

The frequencies of the oscillations are plotted in Fig. 4 as a function of a scaled microwave amplitude $\alpha \equiv (2eV_{\text{ac}}/hf)(C_p/C_\Sigma)$, where V_{ac} is the voltage amplitude of the cw modulation at the pulse gate. The data for $m = 1$ are shown as filled circles; the numbers beside these data points are corresponding microwave power A. The data for $m = 0$ and 2 are also plotted as filled and empty squares, respectively. The experimental results agree with the expected Bessel-function dependence $\hbar\Omega_{\text{Rabi},m} = E_J J_m(\alpha)$. Although $\Omega_{\text{Rabi},0}$ did not reach zero of the Bessel function $J_0(\alpha)$, the observed 0-photon Rabi frequency clearly shows decreases with increasing α. This decrease is a manifestation of the so-called coherent destruction of tunneling [5]. In the plot, we fixed the vertical scale of the Bessel functions to the frequency of the coherent oscillations at $\alpha = 0$ [9]. This frequency is consistent with the result of the spectroscopic measurement of E_J. And α corresponding to the experimental data were calculated according to the transmission loss of the cw signal at $f = 20$ GHz, where the loss was determined by analyzing the power dependence of photon-assisted Cooper-pair tunneling current [17]. Therefore, there is no free parameter in the comparison between the measured and calculated Rabi frequencies.

In conclusion, we observed Rabi oscillations for 0-, 1-, and 2-photon resonances in a Cooper-pair box under strong microwave irradiation. The oscillation frequencies depend on the microwave field amplitude through a Bessel function of the corresponding order. These observations demonstrate coherent control of the quantum state of the individual two-level system by using pulse-modulated microwaves with an arbitrary pulse length and/or microwave amplitude. Moreover, this work opens possibilities of further studies on the fidelity of pulse operation, the effect of decoherence, and the influence of the oscillating driving field on decoherence.

*On leave from Lebedev Physics Institute, Moscow 117924, Russia.

[1] C. Zener, Proc. R. Soc. London A **137**, 696 (1932).
[2] I. I. Rabi, Phys. Rev. **51**, 652 (1937).
[3] See, for example, U. Weiss, *Quantum Dissipative Systems* (World Scientific, Singapore, 1999), 2nd ed.
[4] See articles in Fortschr. Phys. **48**, No. 9–11 (2000).
[5] M. Grifoni and P. Hänggi, Phys. Rep. **304**, 229 (1998).
[6] Yu. Makhlin, G. Schön, and A. Shnirman, Rev. Mod. Phys. **73**, 357 (2001).
[7] V. Bouchiat, D. Vion, P. Joyez, D. Esteve, and M. H. Devoret, Phys. Scr. **T76**, 165 (1998).
[8] Y. Nakamura, C. D. Chen, and J. S. Tsai, Phys. Rev. Lett. **79**, 2328 (1997).
[9] Y. Nakamura, Yu. A. Pashkin, and J. S. Tsai, Nature (London) **398**, 786 (1999); Physica (Amsterdam) **280B**, 405 (2000).
[10] A. Shnirman, G. Schön, and Z. Hermon, Phys. Rev. Lett. **79**, 2371 (1997).
[11] L. Allen and J. H. Eberly, *Optical Resonance and Two-Level Atoms* (Wiley, New York, 1975).
[12] C. P. Slichter, *Principles of Magnetic Resonance* (Springer-Verlag, New York, 1990), 3rd ed.
[13] C. Cohen-Tannoudji, J. Dupont-Roc, and G. Grynberg, *Atom-Photon Interactions: Basic Processes and Applications* (Wiley, NewYork, 1992), Chap. 6.
[14] Though we retain the name, this problem is slightly different from the original Rabi problem (Ref. [2]), where ω_1 is 0 and a circularly polarized driving field couples to the two-level system via $\sigma_x \pm i\sigma_y$ terms.
[15] See e.g., A. Barone and G. Paternò, *Physics and Applications of the Josephson Effect* (Wiley, New York, 1982).
[16] Y. Nakamura and J. S. Tsai, J. Low Temp. Phys. **118**, 765 (2000).
[17] Y. Nakamura and J. S. Tsai, J. Supercond. **12**, 799 (1999).